Results in Optics 21 (2025) 100826

Contents lists available at ScienceDirect

Results in Optics

journal homepage: www.sciencedirect.com/journal/results-in-optics

Mathematical modeling and experimental validation of optical coupling efficiency in Ultraviolet-C light emitting diode systems

Muhammad Salman Mohsin[a,*], Mariana Lanzarini-Lopes[a], Katrina Fitzpatrick[b]

[a] Environmental and Water Resource Engineering, Department of Civil and Environmental Engineering, University of Massachusetts Amherst, MA 01003, United States
[b] Optical Waters Limited, Amherst, MA 01002, United States

ARTICLE INFO

Keywords:
Coupling efficiency
Multimode optical fiber
Ultraviolet
Light emitting diodes

ABSTRACT

This study provides a novel mathematical model for predicting the coupling efficiency (C.E) between multimode optical fibers (MMF) and ultraviolet light-emitting diodes (UV-C LEDs) with a high degree of accuracy. Unlike previous models, which rely on simplified assumptions (ideal conditions), this approach incorporates real-world variations in LED emission profiles, optical misalignments, and Fresnel losses. The model was validated using four distinct optical system configurations, demonstrating strong agreement ($R^2 = 0.94$) with experimental data. The results from this study provide a robust framework for designing efficient UV delivery systems, particularly for disinfection and sensing applications and will serve as a practical guideline that may be useful for both the scientific and industrial community.

1. Introduction

Optical fiber systems are used in a variety of applications such as telecommunication, medicine, automobile, military, lighting industry and environmental remediation (Lanzarini-Lopes et al., 2020; Nair and Dhoble, 2015; Sabri et al., 2015; Uysal and Nouri, 2014; Zhao et al., 2023a, Zhao et al., 2023b). Various light sources can be used in an optical system depending on application. Laser sources enable higher coupling efficiency and are widely used as the accepted light source for most industries. Lasers produce a non-divergent, coherent and monochromatic beam which is ideal for coupling light into optical fibers (Kogelnik & Li, 1966). However, advancements and market infiltration of light-emitting diodes (LED) are making them an interesting option for use with optical fibers.

Visible LEDs are often coupled with fibers for use in lighting and decorative applications. UV LED coupling to optical fiber is being explored for various applications such as disinfection and optical detection techniques (Belz et al., 2007; Degner et al., 2009; Mohsin et al., 2023). Recently side-emitting optical fibers coupled with UV-C LED (265 nm) were introduced for disinfection and biofilm prevention along with improved light distribution (Alidokht et al., 2024; Lanzarini-Lopes et al., 2019, 2020; Mohsin et al., 2024; Zhao, Rho, et al., 2023). UV-C LEDs with peak at 265 nm range demonstrate highest germicidal efficacy by inducing microbial inactivation through DNA and protein structure damage (Sinha & Häder, 2002). Understanding what effects coupling efficiency of LEDs, specifically UV LEDs to optical fibers can enhance their use for environmental and sensing applications. The loss of power due to coupling for visible light LEDS can be withstood due to the high output efficiencies of the technology (50–80 %). However, as wavelengths drop from 400 nm to 265 nm ranges, the efficiencies of UV LEDs drop to (1–3 %) (Beck et al., 2017). Therefore, increasing coupling efficiency can have a substantial impact on the success of UV-C LED and side-emitting optical fiber market infiltration.

C.E is a major factor in any coupling optical system and is influenced by components, misalignment, Fresnel reflection losses and lens aberration (J. Chen et al., 2017). LEDs are incoherent sources of light (Bourget, 2008; Malacara-Hernadez, n.d.). The radiation pattern emitted by the bare LED is known as the Lambertian pattern explained in detail in later section (Lambert & Anding, 1760; Zhenrong et al., 2009). LEDs mostly have a high divergence angle (120^0-130^0 degrees) perpendicular to the junction plane and optical fiber usually used are of small numerical aperture (0.20 to 0.39) (Vidal et al., 2009). Recently a lot of work has been done on increasing the output efficiency of UV-C LEDs by ultrathin tunneling junction and other techniques (Liu et al., 2024; Zhang et al., 2025; Zhou et al., 2024). Fundamental principles of the optic state that only a small fraction of the radiation emitted by the LED would be coupled into the optical fiber due to this mismatch (Yang & Kingsley, 1975). Optical fibers work on the principles of total internal

* Corresponding author.
E-mail address: muhmohsin@umass.edu (M.S. Mohsin).

https://doi.org/10.1016/j.rio.2025.100826
Received 29 January 2025; Received in revised form 22 March 2025; Accepted 8 April 2025
Available online 10 April 2025

Table 1
List of abbreviations.

N.A	Numerical Aperture
$\theta^{'}$	Half of maximum scattering angle of the LED
θ	Plane Acceptance Angle of Fiber
Ω_a	Solid Acceptance Angle of Fiber
T	Transmission Coefficient of Fiber
A_s	Cross-sectional area of LED
A_f	Cross-sectional area of Fiber
n_0	Refractive index of dielectric between LED and Fiber
L	Distance between LED and Fiber
P_f	Power into Fiber
P	Irradiated Power of LED
η	Coupling Efficiency

reflection (TIR), thus a light wave entering the end of the fiber will propagate through the fiber only if the incidence angle is lower than the critical angle of the fiber (Palmer et al., 1983).

Studies have been conducted previously on coupling LEDs to optical fibers with an emphasis on increasing the C.E of the optical system. Some of the common coupling techniques include butt coupling, and the use of collimation lenses and microlenses. (Hudson, 1974; Li et al., 2019; Park et al., 1999; Sun et al., 1991; Wilson, 1998; Yang & Kingsley, 1975). Other studies suggest embedding the light source into the fiber end which has the potential of high light extraction/coupling (J.-J. Chen et al., 2012; Zhenrong et al., 2009). Recently, there have been studies which showed that coupling efficiency can be increased using grating-enhanced and nano-printed microstructures on waveguides end facet (Gu et al., 2022; Yermakov et al., 2023; Zeisberger et al., 2024). Additionally, there is no consensus on which technique would provide maximum C.E and differs on type of application.

Previous studies on coupling efficiency focused primarily on idealized conditions, assuming perfect alignment and ignoring attenuation losses and lens effects. While these models provided theoretical insights, their predictions often deviate from experimental observations, particularly for UV-C LEDs operating at low efficiencies. In this work, we develop and experimentally validate a new mathematical framework that accounts for non-ideal factors, enabling accurate predictions across multiple configurations in real world practical scenarios.

2. Materials and methods

2.1. Development of a novel mathematical model for coupling efficiency

Light-emitting diodes (LED) are considered as Lambertian emitters meaning each point of the LED emits light uniformly in all directions and is independent of angle and position to a surface (Hudson, 1974). If the LED is considered a planar source in two-dimensional space (Fig. 1). Then power is expressed as

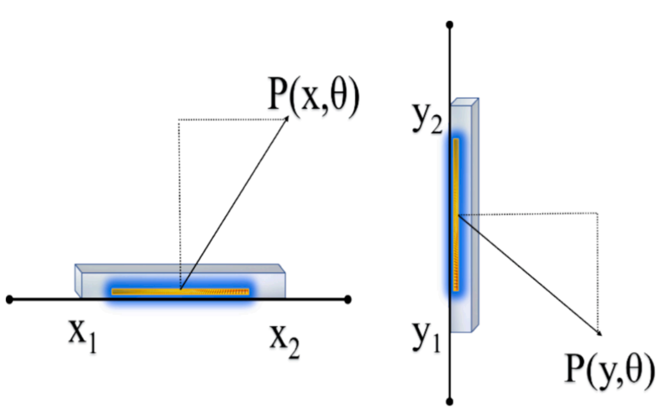

Fig. 1. Radiation expressed in one dimensional space.

P (x, θ) = P.
P (y, θ) = P.

The LED appears to have uniform brightness across its surface. The intensity from any point on the surface of LED decreases by the cosine of the emission angle ($I = I_0 \cos\theta$) with respect to normal. The solid angle decreases in a similar way by the same amount (Lambert & Anding, 1760). Additionally, the ratio between power and solid angle remains constant across the surface of the LED. Therefore, irradiance is constant with respect to angle and position and can be written as equation (1).

$$I_{LED} = \frac{P}{\Omega_{max} A_s} \tag{1}$$

(Hudson, 1974) in their model used a similar equation to quantify the rate of change of power across the phase volume of a light source. In Eq. (2) Ω_{max} (steradian) is the solid angle (explained later in detail Fig. 2 (b)) subtended by the LED on the MMF interface and is equal to $\pi sin^2\theta'_{max}$ (Arecchi et al., 2007). P (mW) is the power of the LED, θ'_{max} (radian) is the half of maximum scattering angle of the LED and A_s (mm^2) is the cross-sectional area of the LED .

$$I_{LED} = \frac{P}{\pi\, sin^2\theta'_{max} A_s} \tag{2}$$

When an LED is coupled to a waveguide although the irradiance emitted by the LED is uniform the power coupled at the interface of the waveguide changes with respect to the solid angle of the waveguide and LED (Fig. 2(a)).

The numerical aperture (N.A) of the fiber is defined as the sine of the largest angle an incident ray can have for total internal reflection in the core of the fiber. The maximum acceptance angle θ for optical fibers is calculated by Snell's Law using the following equation:

$$N.A = \eta_0 sin\theta = \sqrt{\eta_1^2 - \eta_2^2}\eta 1 > \eta 2 \tag{3}$$

Where η_0 (air = 1) is the refractive index of air in between fiber and light source, η_1 and η_2 are the refractive indices of the core and cladding of the fiber. When calculating the C.E of optical fibers, the solid angle must also be taken into consideration. The effective solid acceptance angle is the maximum angle that light emitted from the LED will enter and be internally reflected through the fiber. Only a portion of the light emitted by a LED is within the effective solid acceptance angle of the fiber, therefore limiting the amount of light coupled into the fiber.

Any point on the interface of the fiber will have an effective solid acceptance angle illustrated in (Fig. 2(b)) and calculated in Eq. (6) (Arecchi et al., 2007).

$$\Omega_a = 4\pi \frac{\pi r^2}{4\pi R^2} \tag{4}$$

$$\Omega_a = \frac{\pi r^2}{R^2} (sin\theta = \frac{r}{R}) \tag{5}$$

$$\Omega_a = \pi\, sin^2\theta max \tag{6}$$

In solid angle calculation, $4\pi R^2$ is the area of a sphere, πr^2 is the area of a circle and 4π is the solid angle of the whole sphere.

From Fig. 2(b) we can calculate the power coupled into the fiber as.

$$P_f = TI_{LED}\eta_0 A_f \Omega_a \tag{7}$$

Substituting Eq. (2) and (6) into Eq. (7), results in the following equation.

$$P_f = \frac{TPA_f\eta_0\pi\, sin^2\theta_{max}}{A_s\pi sin^2\theta'_{max}} \tag{8}$$

A_f (mm^2) is the cross-sectional area of the fiber, Ω_a (steradian) is the solid acceptance angle of the fiber, T is the transmission coefficient which is a measure of how much light passes through the fiber and is dimensionless (the Fresnel losses which are approximately 4 % at the

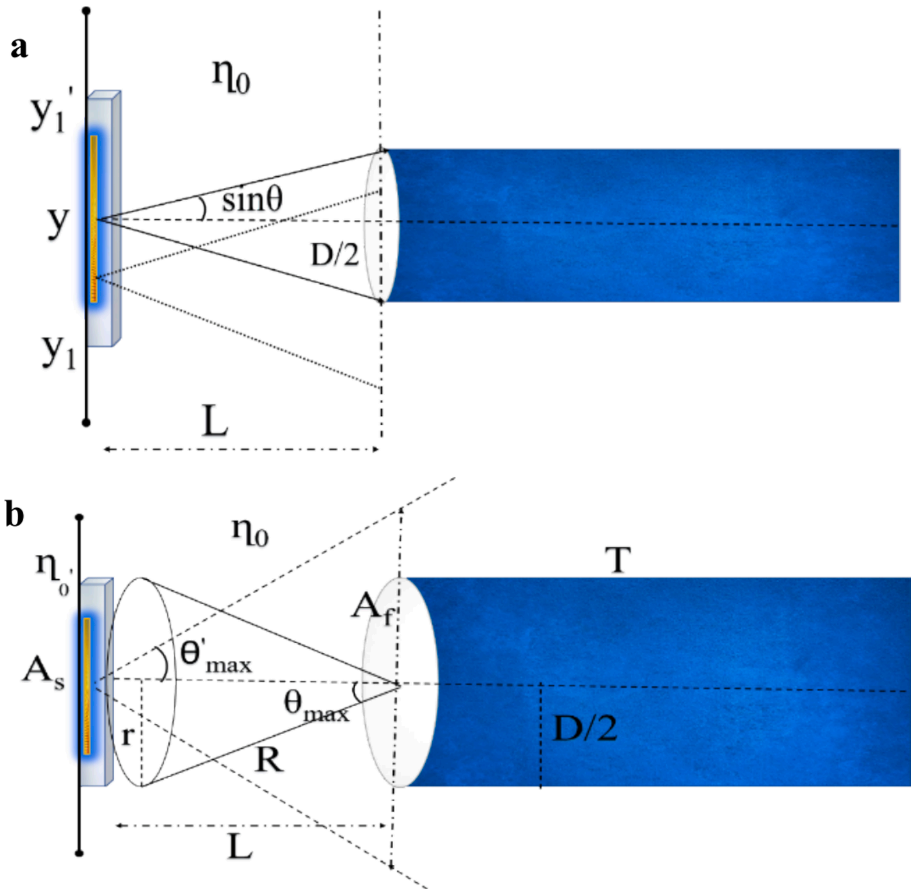

Fig. 2. Illustration showing (a) radiation emitted by each point of the LED onto the fiber interface. Point y which is centrally aligned couples more light into the fiber as compared point y1 on the edge. (b) Effective solid acceptance angle of the multimode optical fiber.

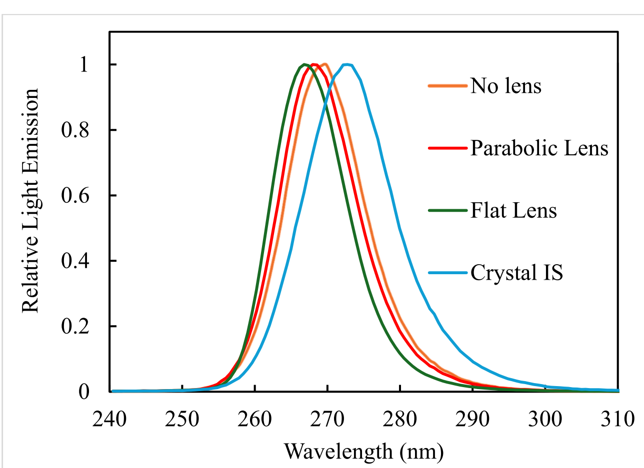

Fig. 3. Relative light emission spectrum of the UV-C LEDs with a full-width half-max (FWHM) of approximately 13 nm.

air-glass interface due to reflection are taken into account and T = 0.96, assuming all of the incident light is focused in), A_s (mm^2) is the cross-sectional area of the light source.

For simplicity, we consider the scenario where the light is incident perpendicularly, and the centers of the LED and optical fiber are aligned. Cases with oblique incidence, where the light enters at an angle and the centers of the LED and optical fiber do not align, are not taken into account.

Lastly, light from an unfocused source follows inverse square law which states that light intensity decreases as the distance between the source and the receiver increases. The rate of decrease is inversely proportional to the square of the distance between them (Brownson, 2014a). Thus, by decreasing the distance between the LED and MMF the C.E could be increased and vice versa. An important consideration to keep in mind is that light intensity decreases by a factor of L^2 which is the distance between the LED and the MMF and is a dimensionless term. Incorporating L^2 into Eq. (8).

$$P_f = \frac{TPA_f\eta_0\pi \sin^2\theta_{max}}{A_sL^2\pi \sin^2\theta'_{max}} \tag{9}$$

P_f (mW) is the power that would be coupled into the fiber (see Table 1). Hence C.E could be calculated by taking a ratio of the power coupled into the fiber and total power coming out of the LED.

$$\eta = \frac{\text{Power into fiber}}{\text{Irradiated Power of LED}} = \frac{P_f}{P} \tag{10}$$

2.2. Coupling UV-C LED to optical fiber

Four types of UV-C LED were used in this study, each with different radiation angle, power, size and encapsulating lenses (Flat lens, parabolic lens and no lens from Boston Electronics and no lens from Crystal IS) (Table 2). All UV-C LEDs were 265-275 nm wavelength (Fig 3). Three different sizes of MMF (0.6 mm, 1 mm and 1.5 mm) with a numerical aperture of 0.39 from Thorlabs were used in this study for comparative analysis (FT600UMT, FT1000UMT, FT1500UMT). The optical system which yielded the maximum C.E was also tested with a higher N.A (0.50) fiber (FP600URT, FP1000URT, FP1500URT). A 7-fiber bundle made of 1 mm diameter fibers was also tested to measure its effects on C.E when

Table 2
Specification of the four LEDs used in this study.

LED Type	Manufacturer	Viewing Angle (Degrees)	Lens type	Power (mW)	Current (mA)
VPC134-265-C	Boston Electronics	120^0-130^0	Flat Lens	16	350
VC1X1C48L3-265 (Previous Generation)	Boston Electronics	30^0	Parabolic Lens	43	700
VC1X1C48L3-265 (Previous Generation)	Boston Electronics	120^0-130^0	No Lens	43	700
KL265-50 V-SM-WD	Crystal IS	130^0	No Lens	70	500

coupled to each UV-C LED.

The schematic of the experimental set-up used for coupling UV-C LED to the optical fiber is illustrated in (Fig. 4). The optical coupling system consisted of a LED which was attached to FC/PC adapter plate (SM1FCA2) and four aluminium heat sinks (8.8 mm^2 x 5 mm) for proper heat dissipation and LED cooling. Kinematic mounts (KS1T-SM1) and M6 optical posts were used for precise alignment of the LED to the optical fiber. A B&K Precision 1715A Single Output Power Supply was used to power the LED. The four types of LEDs selected are the most common commercially used UV-C LEDs.

2.3. Irradiance measurements

All the irradiance measurements were taken using a spectroradiometer (AvaSpec-2048L, Avantes, Louisville, CO USA). The spectroradiometer was adjusted to measure irradiance from 240 to 300 nm. The sensor tip (0.119 cm^2) was placed parallel and flushed to the MMF terminal end and aligned centrally with precision for accurate measurements. Active alignment ensured the highest output and therefore accurate alignment was recorded during each replicate. All the light intensity/irradiance measurements for each LED and MMF were taken in the open air on top of an optical bench in the laboratory. The intensity (mW/cm^2) was measured by placing the sensor tip parallel and flushed to the junction plane of the fiber. Triplicate measurements were taken for each step of this study.

2.4. Attenuation measurements

Attenuation (α (dB/cm)) described by the Beer-Lambert Law (Swinehart, 1962), relates I_T to the material properties and geometry of the optical fiber it is passing through.

$$\alpha\ (\mathrm{dB/cm}) = -10\log\left(\frac{I_T}{I_0}\right)/L \tag{11}$$

Attenuation was quantified by the cutback method (Hui & O'Sullivan, 2009) using Eq. (11), where a 10 cm fiber was cut 3 times to 8, 6, and 4 cm. The transmittance was measured for each length (L) and reported with reference to the transmittance at the 4 cm fiber (I_0).

2.5. Coupling method

In geometrical optics, it follows that if the ratio of fiber cross-sectional area to the LED radiation emitting area is ≤ 1, then C.E is maximum by butt coupling and cannot be improved using collimating optics and when the ratio is > 1C.E could be increased using collimating optics (Hudson, 1974). Therefore, butt coupling and collimation lensed LEDs were used for every diameter fiber. In butt coupling technique the waveguide is attached directly to the light source (diode) with no encapsulating lens or collimation lens in between them. LEDs are incoherent sources of light which follow inverse square law where light intensity is inversely proportional to the distance from source to object (Brownson, 2014b). Thus, it is reasonable to assume that more light could be coupled into the fiber by removing the encapsulating lens of the LED and directly butting the fiber to the diode. The second technique was the use of a encapsulated collimation lens to focus more light into the fiber. The C.E was measured with two LEDs with encapsulating lenses including a flat lens and parabolic lens LEDs and two LEDs with no encapsulating lenses, named no lens. The optical fibers were flushed against each of the LED to minimize the distance between the light source and wave guide.

2.6. Bundling of fibers

To measure the effect of bundling of fibers on C.E, fiber bundles were coupled with each LED. A 7-fiber circular bundle of 1 mm diameter fibers was used in this study. Hexagonal packing provides tighter bundling and higher cross-sectional area however circular fibers are a more commonly used fiber geometry. The fibers were arranged in circular rows as shown in (Fig. 5) with a central fiber and 6 surrounding fibers.

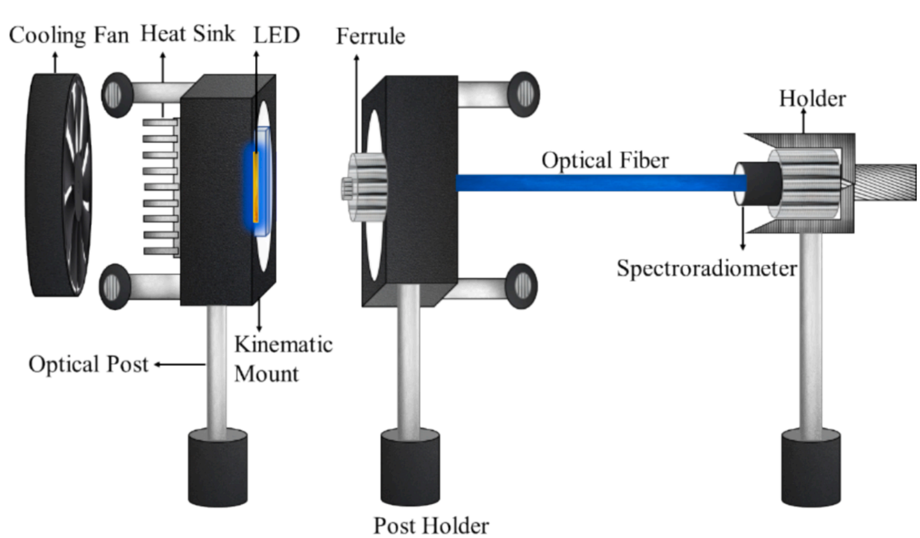

Fig. 4. Schematic of UV-C LED coupled to an optical fiber. The schematic illustrates mounted UV-C LED in alignment with the MMF and spectroradiometer.

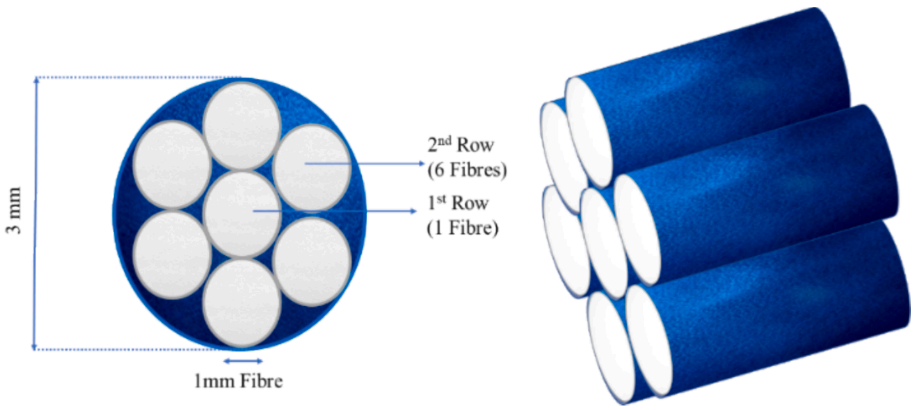

Fig. 5. Schematic of seven fiber bundle arrangement in circular packing.

3. Results and discussion

3.1. Validation of the mathematical model

The C.E was measured for two encapsulated (Flat lens, Parabolic lens) and two no lens (bare diode) UV-C LEDs with 0.6 mm, 1 mm, 1.5 mm diameter fibers and a 7-fiber bundle (1 mm) which have a N.A of 0.39. Fig. 7(a) shows comparative data illustrating the change in C.E with different UV-C LEDs. The C.E was 2.21 ± 0.2 %, 5.77 ± 0.35 %, 9.89 ± 0.06 % and 5.55 ± 0.16 % with 0.6 mm, 1 mm, 1.5 mm diameter fibers and a 7 fiber bundle (1 mm) respectively for a flat lens LED. There was a linear increase in C.E from 2.21 ± 0.2 % to 9.89 ± 0.06 % as fiber diameter was increased from 0.6 mm to 1.5 mm which agrees with our model (Eq. (9) and (Hudson, 1974) coupling equation that C.E is directly proportional to cross-sectional area of the fiber. However, the C.E decreased from 9.89 ± 0.06 % for a 1.5 mm fiber to 5.55 ± 0.16 % for a 7 fiber bundle which has a ~ 3 mm diameter because the phase space area of the bundle (~5.45 mm^2) exceeded the phase space area of the encapsulated lens (~4 mm^2). The C.E can only increase using a fiber bundle when the phase space area of the bundle remains smaller than the phase space area of the LED (Hudson, 1974). Furthermore, as illustrated in Fig. 6 (left); majority of the incident light focused on the outer fibers of the 7 fiber bundle exceeded the N.A of the fibers and is refracted outward, only the incident light focused on the central fiber is within N.A of the fiber and is totally internally reflected; that is why the C.E of single 1 mm fiber (5.77 ± 0.35 %) is approximately same as C.E of the 7 fiber bundle (5.55 ± 0.16 %).

For a parabolic lens LED from Boston Electronics, a linear increase in C.E was also observed with increase in diameter of the fibers at 1.82 ± 0.07 %, 4.53 ± 0.08 % and 13.61 ± 0.42 % for 0.6 mm, 1 mm, 1.5 mm diameter fibers respectively. However, the C.E increased even further when the parabolic lens LED was coupled with a 7-fiber bundle to 16.67 ± 0.90 %. This occurs because the phase space area of the encapsulated parabolic lens (~9 mm^2) was higher than the phase space area of the 7-fiber bundle (~5.45 mm^2) as compared to the flat lens LED. Additionally, a significant amount of the incident light focused on the outer fibers of the 7-fiber bundle was within the N.A of the fibers because the radiant angle of the parabolic LED is 30^0 compared to 130^0 radiant angle of the flat lens LED (Fig. 6-right).

The no lens (bare diode) LED from Boston Electronics follows same trend as flat lens LED, where a linear increase in C.E was observed at 2.83 ± 0.08 %, 11.54 ± 0.07 %, 24.95 ± 0.82 % for 0.6 mm, 1 mm, 1.5 mm diameter fibers and a decrease in C.E at 15.59 ± 1.92 % with a 7-fiber bundle (1 mm) respectively. The decrease in C.E from 24.95 ± 0.82 % for a 1.5 mm fiber to 15.59 ± 1.92 % for a 7-fiber bundle was explained earlier. For single fibers i.e. 0.6 mm, 1 mm, 1.5 mm diameter; highest C.E was achieved by coupling no lens (bare diode) LED from Boston Electronics among all four LEDs. The results showed that butt coupling directly to diode yields higher C.E then coupling to a LED with an encapsulated lens (Flat lens and Parabolic lens). The reason why butt coupling yields higher C.E than encapsulated lens is because a significant portion of light is lost in the first few mm of distance from the diode to the waveguide. Even though the encapsulated lens refracts the incident light trajectory into the waveguide, all of the incident light is not refracted and is lost in dielectric medium in between the light source and the waveguide (Fig. 6). This phenomenon can be seen by comparing the C.E data of the parabolic lens LED with no lens (bare diode) LED from Boston Electronics which is the same LED but without the encapsulated parabolic lens (~3 mm). The C.E increased from 1.82 to 2.83 %, 4.53 to 11.54 % and 13.61 to 24.95 % for 0.6 mm, 1 mm, and 1.5 mm diameter fibers respectively simply by removing the encapsulating parabolic lens which reduced the ~ 3 mm distance between the diode and the waveguide.

Furthermore, to evaluate how high of a C.E can be achieved with this

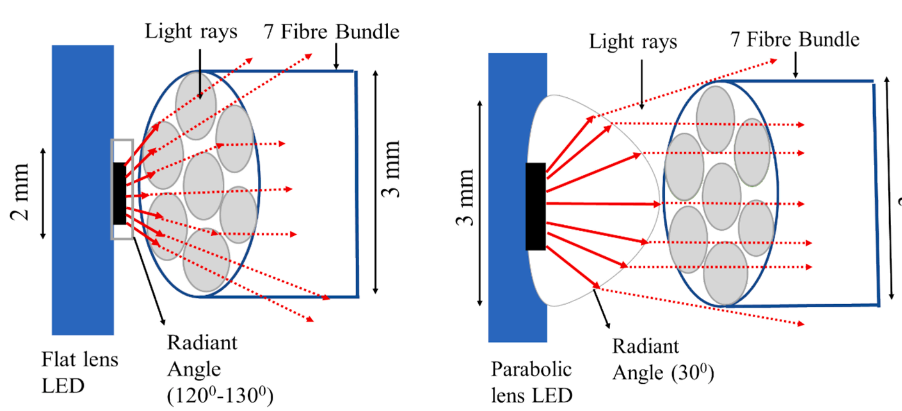

Fig. 6. Schematic of the pathway of light rays from a flat lens and a parabolic lens LED into a 7-fiber bundle.

same configuration; we tested the same no-lens (bare diode) LED with the same diameter fibers but higher N.A (0.5). The C.E increased for all three single fibers i.e., 0.6 mm, 1 mm and 1.5 mm from 2.83 ± 0.08 %, 11.54 ± 0.07 %, 24.95 ± 0.82 % to 11.28 ± 0.4 %, 34.09 ± 1.2 %, and 60.03 ± 0.57 % respectively; when the N.A was increased from 0.39 to 0.50. The C.E increased about 2.5 to 3 times just by increasing the N.A of the fiber by 0.11. The N.A can be increased by using a fiber core material of much higher refractive index than the cladding. When evaluating a 7-fiber bundle for 0.39 and 0.50 N.A, the C.E only increased from 15.59 ± 1.92 %, to 18.55 ± 0.63 %, with no statistical distinction. These results indicated that N.A is not a significant parameter when it comes to enhancing the C.E of a fiber bundle for a no-lens LED not for every LED optical system.

A linear increase in C.E was not observed for the no lens (bare diode) LED from Crystal IS. The C.E increased from 2.48 ± 0.24 % to 6.43 ± 0.38 % for 0.6 mm and 1 mm fiber but no further increase in C.E was observed for 1 mm, 1.5 mm diameter and a 7-fiber bundle. There was no statistically significant difference ($p < 0.05$) in the C.E of 1 mm, 1.5 mm and 7-fiber bundle at 6.43 ± 0.38 %, 7.46 ± 0.25 % and 6.67 ± 0.49 % respectively. The lack of increase of C.E for the 7-fiber bundle was explained earlier but the lack of increase of C.E from 1 mm to 1.5 mm fiber was anomalous and could be due to the trajectory of incident light exceeded the N.A at the edges of the fiber and was refracted outward. Furthermore, the Crystal IS LEDs are fabricated on an aluminum nitride (AlN) substrate, whereas the LEDs from Boston Electronics utilize a sapphire substrate. AlN and sapphire have refractive indices of approximately 2.1 and 1.75, respectively. Given that the optical fiber used in this study has a silica core with a refractive index of 1.45, the sapphire substrate provides a closer refractive index match, potentially resulting in improved optical coupling efficiency at the LED–fiber interface while the AlN substrate LED shows lower coupling efficiency due to a higher refractive index mismatch.

Fig. 7(a) shows experimentally measured data illustrating the change in C.E with different UV-C LEDs along with modelled data. Residual analysis was used to measure the strength of relationship between the experimental data and modelled data indicating a strong correlation ($R^2 = 0.94$) between the two variables (Fig. 7(b)). The data for 1.5 mm fiber with no lens LED from Crystal IS was not included in the residual analysis and was considered anomalous as explained earlier.

Limitations: Some limitations to the model developed in this work include (1) The model is designed for single fiber coupling methods and does not work for fiber bundles and (2) The model is designed for butt coupling mechanism where the fiber is directly attached to the diode or the encapsulating lens, it does not work for collimation lenses with focal lengths placed in between LED and fiber. (3) The model is designed for normal incidence light not for oblique incidence as the coupling

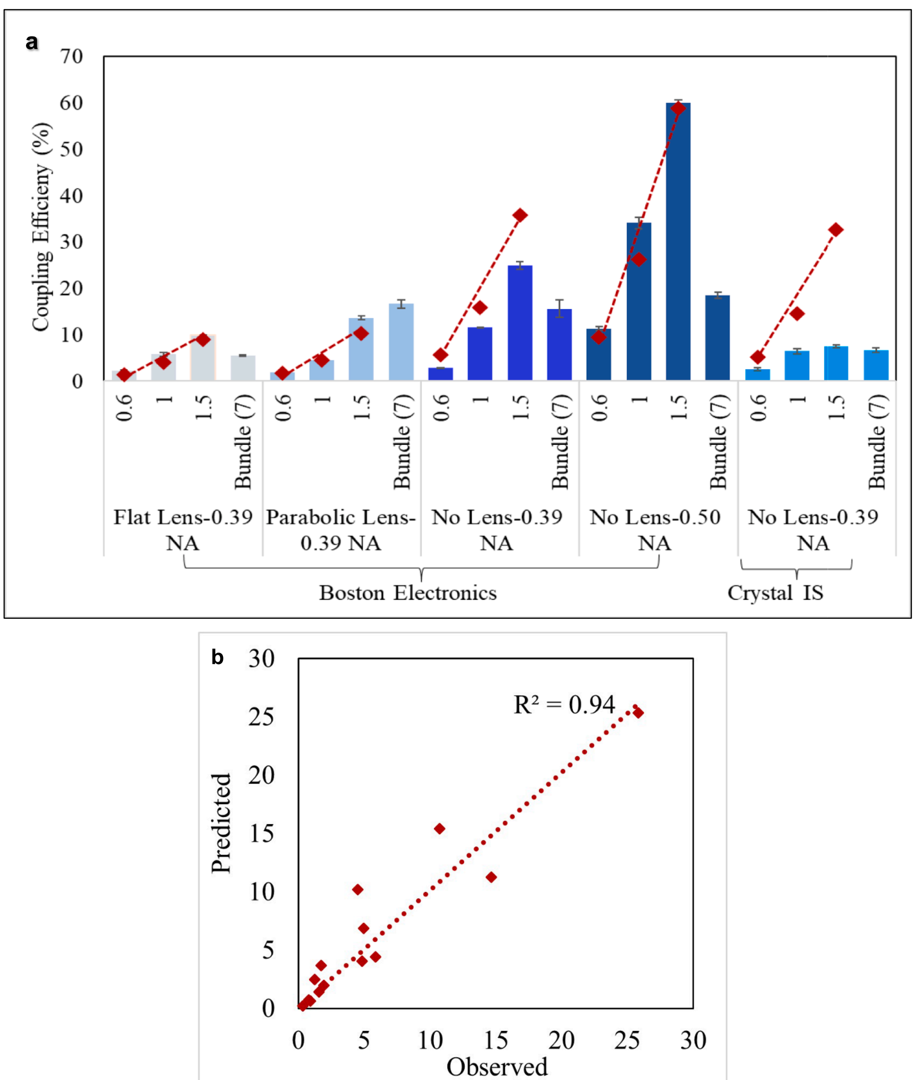

Fig. 7. (a) Coupling efficiency of different fibers with x-axis illustrating diameter of each fiber (mm) coupled with the type of LED and N.A of the fibers. Experimental data is represented by bars () and modelled data is represented by (). (b) Illustrates the fitness of experimental data (observed) vs our modelled data (predicted).

efficiency would be very low due to LED and optical fiber center misalignment. However, recently there have been studies which showed that coupling efficiency can be increased further for oblique incident light with wide angle using grating enhanced and nano printed micro-structures on waveguides(Gu et al., 2022; Yermakov et al., 2023; Zeisberger et al., 2024).

3.2. Comparative analysis with other C.E models

The coupling efficiency between an input field and a waveguide has been explicitly examined in a multitude of literature (Niu & Xu, 2007; Saruwatari & Nawata, 1979; Yermakov et al., 2023b), but most of them have been developed for coherent sources of light (laser beams) with a given Gaussian beam waist size. For incoherent sources like LEDs, parameters like irradiance pattern and angles are used rather than beam waist.

Hudson, 1974 and Yang & Kingsley, 1975 developed C.E models designed for coupling with incoherent light sources (LEDs). Yang & Kingsley, (1975) in their study titled “Calculation of Coupling Losses Between Light Emitting Diodes and Low-Loss Optical Fibers” derived the following model for maximum coupled power without an encapsulating lens.

$$I_{c1} \approx T\Omega_a B[\frac{\pi}{2}D^2 + (2R^2 - D^2)cos^{-1}(\frac{R}{D}) - RD(1 - \frac{R^2}{D^2})^{\frac{1}{2}} + \frac{R}{D^2}(D^2 - R^2)^{\frac{3}{2}} - \frac{1}{2}R(D^2 - R^2)^{\frac{1}{2}} - \frac{1}{2}D^2 sin^{-1}(\frac{R}{D})] \quad (12)$$

Where T is the transmission coefficient, Ω_a is the fibers angular acceptance angle, B is the source radiance, D is the diameter of the optical fiber and R is the radius of light source. This model assumes $R \leq D$ and was validated against experimental data, yielding a correlation coefficient (R^2) of 0.79 (Fig. 8(a)). Some of the model’s limitations include (1) The model ignores the divergence angle of the LED, which can significantly affect coupling efficiency, especially for Lambertian sources like UV-C LEDs. (2) The model assumes zero distance between the LED and the fiber, implying perfect alignment and no light losses due to separation unrealistic conditions in practical setups.

Hudson., (1974) in his study titled “Calculation of the Maximum Optical Coupling Efficiency into Multimode Optical Waveguides” also created a model to calculate maximum C.E from an LED into a multimode optical fiber.

$$E_c(max) = \frac{(A_f(N.A)2)}{(A_s n_0^2)} \quad (13)$$

Where E_c(max) is the maximum C.E, A_f is the fiber cross-sectional area, A_s is the LED cross-sectional area, N.A is the numerical aperture of the fiber and n_0 is the refractive index of the dielectric medium in between light source and optical fiber (air). This model demonstrated better correlation with experimental data (R2 = 0.86) compared to Yang & Kingsley’s (1975) approach. (Fig. 8(b)). While this approach provides a basic framework and was much simpler than the previous model; some of the model’s limitations include (1) it also does not take into account the radiant angle of the light source (2) the model assumes ideal conditions when $A_s \leq A_f$ almost all of the light is focused into the fiber (3) the model does not take into account distance between the light source and fiber overlooking inverse-square law losses.

Our study addresses the limitations of these earlier models by developing a new mathematical framework that incorporates (1) Radiant angle dependency-Unlike previous models, our approach explicitly accounts for LED divergence angles, making it more accurate for modern UV-C LEDs, which inherently exhibit high beam spread. (2) Distance effects on efficiency-The model includes distance dependence between the LED and fiber, accounting for inverse-square law losses; a key factor overlooked in prior studies. (3) Refractive index of the encapsulated lens-The model includes the refractive index of the LED encapsulating lens accounting for the deviation in radiant angle. (e.g the parabolic lens LED has an encapsulated lens of fused quartz withn_0 = 1.49). (4) Experimental validation and accuracy- Residual analysis of the current model demonstrated a significantly higher correlation (R^2 = 0.94) with experimental data compared to previous models, proving its predictive reliability across diverse setups. (5) Sensitivity analysis- By performing sensitivity tests on parameters such as fiber diameter, N.A., and LED emitting area, our model provides a design tool for optimizing coupling efficiency without requiring exhaustive experimental trials.

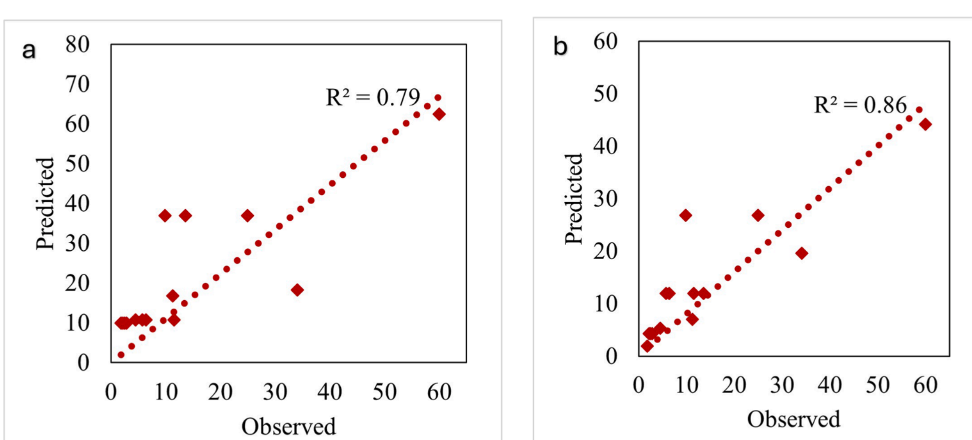

Fig. 8. (a) Illustrates the correlation coefficient of Yang & Kingsley’s (1975) modelled data (predicted) vs our experimental data (observed) (b) Illustrates the correlation coefficient of Hudson., (1974) model modelled data (predicted) vs our experimental data (observed).

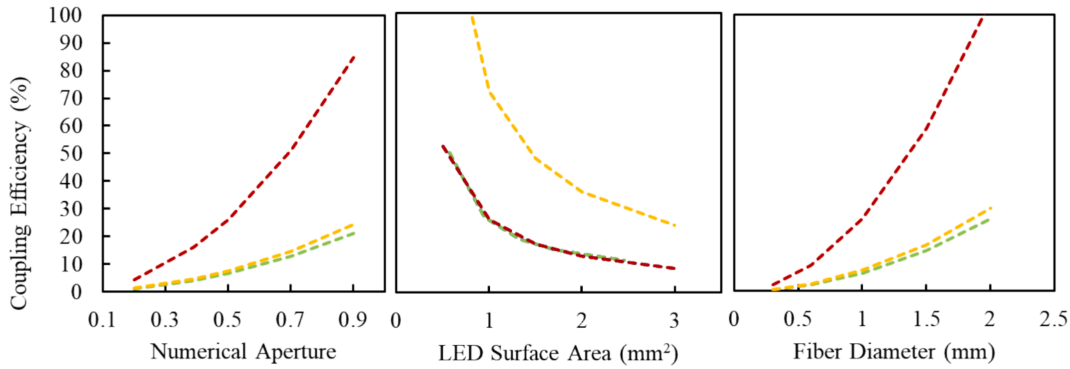

Fig. 9. Coupling efficiency as a function of numerical aperture, LED surface area and fiber diameter for a no-lens (red), flat lens (green) and parabolic lens (yellow) UV-C LED specifications.

3.3. Sensitivity analysis on different parameters affecting C.E

The model equation shows how increase in transmission coefficient (T), power of LED (P), fiber cross-sectional area (A_f) and θ (fiber acceptance angle) will lead to higher power coupled into the fiber while increase in LED cross sectional area (A_s), distance between LED and fiber (L) and $\theta^{'}$ (LED scattering angle) will decresease the power coupled into the fiber. A sensitivity analysis was perfomed on the numerical aperture (N.A), LED cross-sectional area (A_s) and fiber diameter to visualize the impact that these parameters can have on C.E (Fig. 9). All other parameters were kept constant in reference to the light source (no lens, flat lens and parabolic lens LED separately) and N.A was varied from 0.2 to 0.9, LED cross-sectional area was varied from 0.5 to 3 mm^2 and fiber diameter was varied from 0.3 mm to 2 mm to encompass most of the commercially available MMF coupled with LEDs. The results showed that increasing the N.A and fiber diameter would increase the C.E of the system but upto our knowledge 0.50 N.A and 1.5 mm fiber diameter are the maximum fibers available commercially. Conversely, decreasing the LED surface area from 1 to 0.5 mm^2 would increase the C.E of the system but the smallest commercially available LED have surface area of approximately 1 mm^2. Therefore, practically maximum C.E (59 %) could be achieved by using a 1.5 mm diameter fiber with a N.A of 0.50 coupled with a 1 mm^2 no lens LED. The experimentally measured data was in conformation with the model-predicted data and showed a C.E of (60 %) with the same optical system configuration.

Lastly, the attenuation in fibers was measured out to be 0.132 ± 0.035 dB/cm for 265 nm wavelength using Eq. (11). A significant amount of light is being lost to intrinsic characteristics (material) of the fiber (Swinehart, 1962), which shows the significance of wavelength specific fibers for coupling purposes which are designed to transmit that wavelength. These fibers have a wavelength range of 300 to 1200 nm.

4. Conclusions

This study presents a novel mathematical model for coupling efficiency between UV-C LEDs and multimode optical fibers, validated across multiple configurations. Unlike previous models, this approach incorporates practical factors such as beam divergence, Fresnel losses, inverse square law, and attenuation, achieving an R^2 of 0.94 with experimental data. These findings establish the model as a design tool for optimizing optical coupling systems, providing a foundation for further studies involving advanced optics and microstructures.

CRediT authorship contribution statement

Muhammad Salman Mohsin: Writing – review & editing, Writing – original draft, Visualization, Validation, Methodology, Investigation, Formal analysis, Data curation, Conceptualization. **Mariana Lanzarini-Lopes:** Writing – review & editing, Supervision, Funding acquisition. **Katrina Fitzpatrick:** Writing – review & editing, Investigation, Data curation.

Funding

This work was funded by the University of Massachusetts Manning/ IALS Innovation Grants phase I and II.

Declaration of competing interest

Mariana Lanzarini-Lopes reports a relationship with Optical Waters that includes board membership, equity or stocks, and funding grants. Katrina Fitzpatrick reports a relationship with Optical Waters that includes board membership, equity or stocks, and funding grants.

Data availability

Data will be made available on request.

References

Alidokht, L., Fitzpatrick, K., Butler, C., Hunsucker, K.Z., Braga, C., Maza, W.A., Fears, K. P., Arekhi, M., Lanzarini-Lopes, M., 2024. UV emitting glass: A promising strategy for biofilm inhibition on transparent surfaces. *Biofilm* 7, 100186. https://doi.org/10.1016/j.bioflm.2024.100186.

Arecchi, A. V., Messadi, T., & Koshel, R. J. (2007). *Field Guide to Illumination*. SPIE. https://doi.org/10.1117/3.764682.

Beck, S.E., Ryu, H., Boczek, L.A., Cashdollar, J.L., Jeanis, K.M., Rosenblum, J.S., Lawal, O.R., Linden, K.G., 2017. Evaluating UV-C LED disinfection performance and investigating potential dual-wavelength synergy. *Water Res.* 109, 207–216. https://doi.org/10.1016/j.watres.2016.11.024.

Belz, M., Klein, F.A., Eckhardt, H.S., Klein, K.-F., Dinges, D., Grattan, K.T.V., 2007. Optical detection techniques and light delivery with UV {LEDs} and optical fibres. *J. Phys. Conf. Ser.* 85, 12034. https://doi.org/10.1088/1742-6596/85/1/012034.

Bourget, C.M., 2008. An Introduction to Light-emitting Diodes. *HortSci.* 43 (7), 1944–1946. https://doi.org/10.21273/HORTSCI.43.7.1944.

Brownson, J. R. S. (2014a). Laws of Light. In *Solar Energy Conversion Systems* (pp. 41–66). Elsevier. https://doi.org/10.1016/B978-0-12-397021-3.00003-X.

Brownson, J. R. S. (2014b). Laws of Light. In *Solar Energy Conversion Systems* (pp. 41–66). Elsevier. https://doi.org/10.1016/B978-0-12-397021-3.00003-X.

Chen, J., Loeb, S., Kim, J.H., 2017. LED revolution: Fundamentals and prospects for UV disinfection applications. *Environ. Sci. Water Res. Technol.* 3 (2), 188–202. https://doi.org/10.1039/c6ew00241b.

Chen, J.-J., Wang, T.-Y., Huang, K.-L., Liu, T.-S., Tsai, M.-D., Lin, C.-T., 2012. Freeform lens design for LED collimating illumination. *Opt. Express* 20 (10), 10984. https://doi.org/10.1364/OE.20.010984.

Degner, M., Damaschke, N., Ewald, H., O'Keeffe, S., Lewis, E., 2009. UV LED-based fiber coupled optical sensor for detection of ozone in the ppm and ppb range. *IEEE Sensors* 2009, 95–99. https://doi.org/10.1109/ICSENS.2009.5398230.

Gu, Y., Wang, N., Shang, H., Yu, F., Hu, L., 2022. Investigations on Grating-Enhanced Waveguides for Wide-Angle Light Couplings. *Nanomaterials* 12 (22), 3991. https://doi.org/10.3390/nano12223991.

Hudson, M.C., 1974. Calculation of the Maximum Optical Coupling Efficiency into Multimode Optical Waveguides. *Appl. Opt.* 13 (5), 1029. https://doi.org/10.1364/ao.13.001029.

Hui, R., O'Sullivan, M., 2009. Chapter 4 - Optical Fiber Measurement. In: Hui, R., O'Sullivan, M. (Eds.), *Fiber Optic Measurement Techniques*. Academic Press, pp. 365–479.

Kogelnik, H., Li, T., 1966. Laser Beams and Resonators. *Appl. Opt.* 5 (10), 1550. https://doi.org/10.1364/AO.5.001550.

Lambert, J. H., & Anding, E. (1760). Photometria, sive De mensura et gradibus luminus, colorum et umbrae. In *Leipzig : W. Engelmann* (Augustae V). Augustae Vindelicorum [Augsburg] : sumptibus vidvae Eberhardi Klett..., 1760. https://doi.org/https://doi.org/10.3931/e-rara-9488.

Lanzarini-Lopes, M., Garcia-Segura, S., Hristovski, K., Messerly, M., Simon, A.J., Westerhoff, P., 2019. Particle-modified polymeric cladding on glass optical fibers enhances radial light scattering. *J. Opt. Soc. Am. B* 36 (6), 1623. https://doi.org/10.1364/josab.36.001623.

Lanzarini-Lopes, M., Zhao, Z., Perreault, F., Garcia-Segura, S., Westerhoff, P., 2020. Germicidal glowsticks: Side-emitting optical fibers inhibit Pseudomonas aeruginosa and Escherichia coli on surfaces. *Water Res.* 184, 116191. https://doi.org/10.1016/j.watres.2020.116191.

Li, X., Cai, M., Wang, L., Niu, F., Yang, D., Zhang, G., 2019. Evaluation survey of microbial disinfection methods in UV-LED water treatment systems. *Sci. Total Environ.* 659, 1415–1427. https://doi.org/10.1016/j.scitotenv.2018.12.344.

Malacara-Hernández, Z. (n.d.). Incoherent Light Sources. In *Advanced Optical* Instruments *and Techniques* (pp. 561–578). CRC Press. https://doi.org/10.1201/9781315119977-15.

Mohsin, M.S., Avdic, M., Fitzpatrick, K., Lanzarini-Lopes, M., 2024. UV-C side-emitting optical fiber-based disinfection: a promising approach for infection control in tight channels. *Microbiol. Spectrum*. https://doi.org/10.1128/spectrum.00040-24.

Mohsin, M.S., Fitzpatrick, K., Avdic, M., Fiorentino, J., Lanzarini-Lopes, M., 2023. Low-irradiance inactivation kinetics of *Escherichia coli* during prolonged exposure to ultraviolet-C radiation. *Environ. Sci. Water Res. Technol.* 9 (6), 1654–1662. https://doi.org/10.1039/D2EW00886F.

Nair, G.B., Dhoble, S.J., 2015. A perspective perception on the applications of light-emitting diodes. *Luminescence* 30 (8), 1167–1175. https://doi.org/10.1002/bio.2919.

Niu, J., Xu, J., 2007. Coupling efficiency of laser beam to multimode fiber. *Opt. Commun.* 274 (2), 315–319. https://doi.org/10.1016/j.optcom.2007.02.027.

Palmer, A. W., Croft, J. R., & Valsler, R. (1983). *<title>Potential Applications For Total Internal Reflection Fibre Optic Sensors</title>* (L. R. Baker, Ed.; pp. 206–207). https://doi.org/10.1117/12.934585.

Park, E., Kim, M., & Kwon, Y. (1999). *<00752541.Pdf>*. *11*(4), 439–441.

Sabri, N., Aljunid, S. A., Salim, M. S., & Fouad, S. (2015). *Fiber Optic Sensors: Short Review and Applications* (pp. 299–311). https://doi.org/10.1007/978-981-287-128-2_19.

Saruwatari, M., Nawata, K., 1979. Semiconductor laser to single-mode fiber coupler. *Appl. Opt.* 18 (11), 1847. https://doi.org/10.1364/AO.18.001847.

Sinha, R.P., Häder, D.-P., 2002. UV-induced DNA damage and repair: a review. *Photochem. Photobiol. Sci.* 1 (4), 225–236. https://doi.org/10.1039/b201230h.

Sun, T., Wu, H., Wang, W., 1991. A technique for coupling LEDs to optical fibers. *Sens. Actuators, A* 29 (2), 127–131. https://doi.org/10.1016/0924-4247(91)87114-I.

Swinehart, D.F., 1962. The Beer-Lambert Law. *J. Chem. Educ.* 39 (7), 333. https://doi.org/10.1021/ed039p333.

Uysal, M., Nouri, H., 2014. Optical wireless communications & #x2014; An emerging technology. In: *2014 16th International Conference on Transparent Optical Networks (ICTON)*, pp. 1–7. https://doi.org/10.1109/ICTON.2014.6876267.

Vidal, E., Otaduy, D., González, F., Saiz, J. M., & Moreno, F. (2009). *Design and optimization of a collimating optical system for high divergence LED light sources* (P. Z. Mouroulis, R. B. Johnson, & V. N. Mahajan, Eds.; p. 74280C). https://doi.org/10.1117/12.825287.

Wilson, R.G., 1998. Ball-lens coupling efficiency for laser-diode to single-mode fiber: comparison of independent studies by distinct methods. *Appl. Opt.* 37 (15), 3201. https://doi.org/10.1364/ao.37.003201.

Yang, K.H., Kingsley, J.D., 1975. Calculation of Coupling Losses Between Light Emitting Diodes and Low-Loss Optical Fibers. *Appl. Opt.* 14 (2), 288. https://doi.org/10.1364/ao.14.000288.

Yermakov, O., Zeisberger, M., Schneidewind, H., Kim, J., Bogdanov, A., Kivshar, Y., Schmidt, M.A., 2023. Advanced fiber in-coupling through nanoprinted axially symmetric structures. *Appl. Phys. Rev.* 10 (1). https://doi.org/10.1063/5.0127370.

Zeisberger, M., Schneidewind, H., Wieduwilt, T., Yermakov, O., Schmidt, M.A., 2024. Nanoprinted microstructure-assisted light incoupling into high-numerical aperture multimode fibers. *Opt. Lett.* 49 (8), 1872. https://doi.org/10.1364/OL.521471.

Zhao, Z., Luo, Y.-H., Wang, T.-H., Sinha, S., Ling, L., Rittmann, B., Alvarez, P., Perreault, F., Westerhoff, P., 2023a. Phenotypic and Transcriptional Responses of *Pseudomonas aeruginosa* Biofilms to UV-C Irradiation via Side-Emitting Optical Fibers: Implications for Biofouling Control. *Environ. Sci. Tech.* 57 (41), 15736–15746. https://doi.org/10.1021/acs.est.3c04658.

Zhao, Z., Rho, H., Shapiro, N., Ling, L., Perreault, F., Rittmann, B., Westerhoff, P., 2023b. Biofilm inhibition on surfaces by ultraviolet light side-emitted from optical fibres. *Nat. Water* 1 (7), 649–657. https://doi.org/10.1038/s44221-023-00111-7.

Zhenrong, Z., Xiang, H., Xu, L., 2009. Freeform surface lens for LED uniform illumination. *Appl. Opt.* 48 (35), 6627. https://doi.org/10.1364/AO.48.006627.